ACS APPLIED MATERIALS & INTERFACES

Research Article

www.acsami.org

Efficient Quasisolid Dye- and Quantum-Dot-Sensitized Solar Cells Using Thiolate/Disulfide Redox Couple and CoS Counter Electrode

Ke Meng and K. Ravindranathan Thampi*

School of Chemical and Bioprocess Engineering, University College Dublin, Belfield, Dublin 4, Ireland

Supporting Information

ABSTRACT: For the first time, a quasisolid thiolate/disulfide-based electrolyte was prepared using succinonitrile as a matrix. An optimized configuration of the quasisolid electrolyte contains 5-mercapto-1-methyltetrazole *N*-tetramethylammonium/disulfide/$LiClO_4$/*N*-methylbenzimidazole in the molar ratio of 0.8:0.8:0.1:0.1. Dye-sensitized solar cells fabricated using this quasisolid electrolyte, together with N719 dye-sensitized photoelectrode and CoS counter electrode, attained power conversion efficiencies of 4.25% at 1 sun and 6.19% at 0.1 sun illumination intensities. The optimized quasisolid electrolyte, when introduced to quasisolid CdS quantum-dot-sensitized solar cells, exhibited a power conversion efficiency of 0.94%, despite the fact that CdS absorbs only a small fraction of the visible light, unlike dyes. The encouraging results show the potential for the utilization of the quasisolid thiolate/disulfide-based electrolyte in sensitized solar cells.

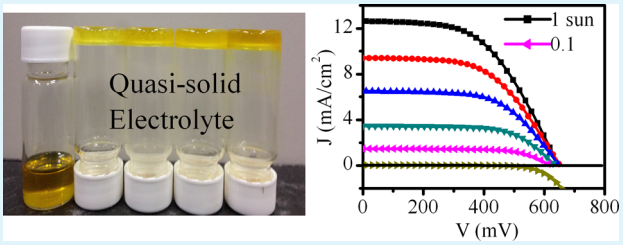

KEYWORDS: *quasisolid solar cell, dye-sensitized solar cell, quantum-dot-sensitized solar cell, thiolate/disulfide redox couple*

1. INTRODUCTION

The third-generation solar cells, including dye-sensitized solar cells (DSSC)[1] and quantum-dot-sensitized solar cells (QDSSC),[2,3] could be potentially produced via roll-to-roll manufacturing lines at lower prices and are adequate for a variety of low-power applications, such as sensors, for example. In these cells, the electrolyte takes the role of charge transport and sensitizer regeneration and the kinetic rate of regeneration is a crucial factor deciding the efficiency of the devices.[4] Electrolytes containing the iodide/triiodide (I^-/I_3^-) redox couple are most commonly used in DSSC;[5] however, its disadvantages include the corrosion of silver-based current collectors and the partial absorption of visible light. This warrants the development of alternative redox electrolytes, which are comparably efficient.[6,7] A thiolate/disulfide (T^-/T_2) redox couple is a promising competitor[8,9] in this regard. DSSC devices containing the T^-/T_2 redox couple have exhibited a promising power conversion efficiency (PCE) of 6.4%.[8] The following studies, including the preparation of proper counter electrode for DSSCs applying T^-/T_2 redox electrolyte[10,11] and the investigation of the T^-/T_2 redox-couple-based ionic liquid electrolytes,[12,13] further suggest that the T^-/T_2 redox couple could replace the I^-/I_3^- in DSSCs, where the latter creates problems for cell stability and longevity.

On the other hand, liquid electrolyte applied in DSSCs has its own engineering and vapor toxicity problems arising from leakages and seal degradation due to volatility of low-boiling solvents, notably certain commonly used liquid nitriles.[14] Thus, different materials were applied to fabricate solid-state DSSCs,[15,16] among which, succinonitrile (SCN) was introduced as a matrix to develop solid-state ionic conductors.[17−19] Succinonitrile is a white clear plastic crystal and is solid at room temperatures, enabling easy handling under ambient conditions, and provides preferable molecular conductivity because of its high concentration of lattice defects.[20] Organic plastic crystals such as SCN exhibit molecular rotational disorders that create defects or vacancies, and these defects or vacancies are thought to support partial translational motion within the lattice, which facilitates molecular/ionic mobility, in general.[21] SCN forms a body-centered cubic plastic phase from 233 K to its melting point at 331 K.[22] In this phase, the rotationally disordered molecules exist in a mixture of three isomeric confirmations, two gauche isomers and one trans isomer, where the trans isomers act as "impurities" in the lattice, creating monovacancies thus lead to high molecular diffusivity.[23] SCN is a nonionic organic plastic crystal with high polarity, which effectively dissolves various types of salts. Dissolving salts in the nonionic SCN matrix provide the mixture with ionic conductivity that originates from the guest salts.[24] The strategy of incorporating SCN matrix with desired salts has been used for various electrochemical devices.[21,22] For example, mixing plastic crystals with lithium compounds has been demonstrated to yield room temperature waxy solids, providing favorable Li^+ ions conductivity, which is attractive to battery applications.[22] SCN possesses similar characteristics in structure and polarity with those commonly used liquid-state organic solvents, such as acetonitrile, valeronitrile, and glutaronitrile, making it a suitable solid-state electrolyte matrix for DSSCs.[21] Grätzel and co-

Received: July 27, 2014
Accepted: November 7, 2014
Published: November 7, 2014

workers mixed SCN with *N*-methyl-*N*-butylpyrrolidinium iodide ($P_{1,4}I$) and iodine to form a solid electrolyte for DSSC with cell efficiencies of around 5% at AM1.5 1 sun illumination.[19] Using the same electrolyte, together with electrospun hierarchically structured TiO_2 nanofiber electrodes, the DSSC performance was improved to 6.54% in full sunlight.[25] Recently, our group has mixed SCN with either 1,2-dimethyl-3-propylimidazoliuum iodide or 1-butyl-3-methylimidazolium iodide ionic liquids for forming a solid, plastic phase electrolyte for DSSCs; cells applying these two electrolytes and a commercial industrial grade dye exhibit power conversion efficiencies of 6.35% and 5.6% at 1 sun, respectively.[17] These results indicate the promising utility of SCN as matrix for efficient quasisolid electrolyte in DSSCs. However, the fact that most of the salts incorporating with SCN are iodides has encouraged us to introduce the alternate thiolate/disulfide redox couple to form an iodine-free quasisolid electrolyte, which is less prone to corrosion.

The commonly used counter electrode material, platinum, is blamed as an inefficient catalytic material to function with this electrolyte.[10] Various kinds of counter electrode materials have been investigated to fabricate DSSCs using the T^-/T_2 redox electrolyte, among which CoS is a promising candidate.[10] Different methods have been employed to fabricate efficient CoS counter electrodes, including electroplating,[26] screen-printing, SILAR,[27] sputtering,[10] or solvothermal techniques.[28] These methods usually require complex instrumentation or are relatively time-consuming. Hence, we have developed a modified SILAR process to fabricate CoS counter electrode for the thiolate/disulfide electrolyte.

In this study, a quasisolid electrolyte was made by mixing a T^-/T_2 redox couple with SCN and complementary CoS counter electrode. The CoS counter electrodes, prepared using a novel method, functionally match the organic redox couple based quasisolid electrolyte. Solar cells incorporating photoelectrodes sensitized by N719 dye, the aforementioned quasisolid electrolyte, and CoS counter electrodes were fabricated. The concentration of the thiolate/disulfide redox couple is varied to maximize the cell performance. Different additives are mixed in the electrolyte to further enhance the power conversion efficiency of cells. DSSCs applying electrolyte containing 0.8/0.8 M T^-/T_2 together with 0.1 M $LiClO_4$ and 0.1 M NMBI in SCN exhibit a promising power conversion efficiency of 4.26% under 1 sun and 6.19% at 0.1 sun illumination intensities. This quasisolid electrolyte is further introduced in CdS QDSSCs, which show a power conversion efficiency of 0.94% under 1 sun irradiation. To the best of our knowledge, this is the first time that a thiolate/disulfide redox-based quasisolid electrolyte has ever been prepared to fabricate sensitized solar cells.

2. EXPERIMENTAL SECTION

2.1. Preparation of Photoelectrodes. The photoelectrodes with TiO_2 films were prepared following a reported procedure.[29] Specifically, a screen-printing method was used to deposit the TiO_2 paste on fluorine-doped tin oxide (FTO) glass substrates in a layer-by-layer manner. In order to suppress back electron transfer, prior to the screen-printing process, a compact TiO_2 underlayer was always deposited onto the FTO substrate. This blocking layer was deposited by a "$TiCl_4$ treatment", which involves the immersion of the FTO substrate into a 40 mM $TiCl_4$ aqueous solution for 30 min at 70 °C.[29] TiO_2 paste was then screen-printed on the $TiCl_4$-treated glass substrate for several cycles. After this, the electrodes were sintered at 325, 375, 450, and 500 °C for 5, 5, 15, and 30 min, respectively. Another $TiCl_4$ treatment was then conducted to deposit a compact TiO_2 over layer on the mesoporous TiO_2 films in order to further reduce charge recombination. Another sintering process was then conducted at 500 °C for 30 min. Two kinds of TiO_2 printing pastes were employed, including a homemade "transparent" paste[29] containing P25 TiO_2 and a "scattering" paste purchased from DyeSol Ltd. (WER 2-0). The electrode configuration used in this study was obtained by depositing seven layers of transparent paste and two layers of scattering paste successively on FTO glass substrates, resulting in the layer thickness of 10 + 5 μm after sintering.

2.2. Sensitization of Photoelectrodes. To obtain N719 dye-sensitized photoelectrodes, bare TiO_2 electrodes were immersed into a dye bath of 5 mM ditetrabutylammonium *cis*-bis(isothiocyanato)bis-(2,2′-bipyridyl-4,4′-dicarboxylato)ruthenium(II) (N719, DyeSol) dye dissolved in a mixed solvent of acetonitrile:*tert*-butyl alcohol:THF (volume ratio 4.5:4.5:1) for 20 h, allowing a saturated dye soak.

To prepare CdS QD-sensitized photoelectrodes, a successive ionic layer absorption and reaction (SILAR) technique was relied on to deposit CdS QDs on the TiO_2 films.[30] The bare TiO_2 electrodes were successively immersed in two different processing solutions for 1 min each: one consisting of 0.5 M $Cd(NO_3)_2$ dissolved in ethanol (3.085 g in 20 mL) and another of 0.5 M Na_2S in methanol/DI water (volume ratio 1:1) (2.4 g $Na_2S{\cdot}9H_2O$ in 20 mL). Following each immersion, rinsing was undertaken for 1 min using the corresponding solvent to remove the excess of each of the precursors, followed by drying under argon. The CdS QD-sensitized electrodes were always passivated with ZnS by dipping alternately into 0.2 M $Zn(NO_3)_2$ in ethanol (1.2 g in 20 mL) and 0.2 M Na_2S in methanol (0.96 g in 20 mL) for 1 min/dip. The dipped electrodes were then rinsed and dried with argon.

2.3. Fabrication of Counter Electrodes. The cobalt sulfide counter electrode introduced in this study was fabricated using a modified SILAR method. First, the FTO substrates were ultrasonically cleaned by detergent solution and acetone. A drop of $Co(NO_3)_2$ solution (10 mM in ethanol) was then deposited on the ultracleaned FTO glass; after air drying, the FTO substrate soaked with Co^{2+} ions were then immersed in a 0.1 M Na_2S methanol solution for 5 s or so to allow the formation of a thin layer of CoS film. Further rinsing and drying under heat gun were conducted to accomplish one SILAR cycle of CoS deposition. By controlling the number of CoS cycles, the thickness of the CoS films can be varied.

2.4. Preparation of the Quasisolid Electrolyte. The T^-/T_2 redox couple was synthesized by following a reported procedure with modifications (the chemical structure of TMAT and T_2 are shown in Figure 1a).[8] Briefly, the 5-mercapto-1-methyltetrazole *N*-tetramethylammonium (TMAT) compound was synthesized by mixing 0.5 g of 5-mercapto-1-methyltetrazole (HT) with 1.8 mL of tetramethylammonium hydroxide (TMAOH) in methanol (25 wt %) under argon with stirring overnight. The resulting solution was vacuum evaporated to obtain the TMAT salt, which was then thoroughly washed with deionized (DI) water and dried under vacuum at 40 °C. The T_2 compound was prepared by oxidization of HT with I_2. Two grams of HT and 1.19 g of K_2CO_3 were dissolved in 20 mL of methanol with the assistance of ultrasonication; 2.18 g of I_2 in 20 mL of methanol was then added dropwise. The mixture was further sonicated for 1 h followed by stirring at room temperature overnight. The T_2 powders were collected through further filtration, followed by drying at 40 °C before use.

To prepare the T^-/T_2-based quasisolid electrolyte, a calculated amount of SCN was melted at 70 °C, followed by adding the corresponding amounts of TMAT and T_2 compounds required. Different kinds of additives, including guanidinium thiocyanate (GuSCN), lithium perchlorate ($LiClO_4$), 4-*tert*-butylpyridine (TBP), or *N*-methylbenzimidazole (NMBI), were added to the solution at 70 °C with stirring to obtain the electrolytes needed. Following the addition of solutes, the mixture was cooled down to obtain the quasisolid electrolyte, as indicated by Figure 1b. No other solvents were involved in the quasisolid electrolyte preparation process.

2.5. Fabrication of Solar Cells. The fabrication of the all-quasisolid solar cells followed a "one-step process" developed earlier.[17] The working electrode and counter electrode were sandwiched

Figure 1. (a) Chemical formula of TMAT/T_2 and (b) photos of the quasisolid electrolytes (leftmost shows the liquid electrolyte applying acetonitrile as solvent).

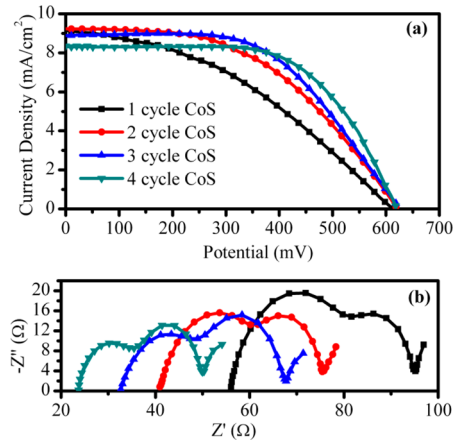

Figure 2. (a) $J-V$ characteristics and (b) Nyquist plots of the DSSCs applying different cycles of CoS films as counter electrode material (cells measured at 1 sun illumination at V vs V_{oc}).

Table 1. Cell Performance Parameters Obtained from $J-V$ Measurements of DSSCs Applying Different Cycles of CoS Films As Counter Electrode Material

CoS cycles	V_{oc} (mV)	J_{sc} (mA/cm^2)	FF (%)	η^a (%)
1	618	9.18	38.50	2.19 ± 0.10
2	619	9.41	47.57	2.78 ± 0.08
3	619	8.93	54.63	3.05 ± 0.09
4	618	8.43	60.80	3.19 ± 0.05
5	618	8.44	56.81	3.03 ± 0.11

[a]The standard deviation of cell efficiency is based on the data of three cells.

together using a Bynel polymer gasket (50 μm thick) to fabricate solar cells. The T^-/T_2-based quasisolid electrolyte was melted at 70 °C first, followed by injecting into the space between the two electrodes through a hole in the counter electrode via vacuum backfilling while the electrolyte remains in its liquid phase. The hole was then sealed with a thin piece (0.1 mm thick) of glass heat-melt-sealed with Bynel.

2.6. Characterizations. Solar cells' photoelectrochemical parameters, including current density/voltage ($J-V$) curves, open circuit voltage (V_{oc}), short circuit current density (J_{sc}), and fill factor (FF), were measured using a Newport 91195A-1000 solar simulator and Newport 69920 arc lamp power supply. The AM 1.5 spectrum with irradiance powers of 1000 W/m^2 was simulated by placing a Newport 81088A air mass filter before the output of the solar simulator. $J-V$ curves and electrochemical impedance spectroscopy (EIS) spectra were recorded with a GAMRY Instruments potentiostat. EIS data was simulated using the electrochemistry software Zview. Incident photon to current conversion efficiency (IPCE) was measured and recorded using a Gilden Photonics IPCE system and software.

3. RESULTS AND DISCUSSION

First, DSSCs were fabricated and characterized to maximize the thickness of CoS films, which was controlled by varying the numbers of CoS layers. The quasisolid electrolyte used in these cells contains 0.4/0.4 M T^-/T_2, respectively, since this is the reported optimized concentration of this redox couple in liquid state electrolyte.[8] The $J-V$ characteristics of the DSSCs applying different cycles of CoS films as counter electrode material are presented in Figure 2a, and the cell parameters obtained from the $J-V$ curves are listed in Table 1. As the number of CoS layers increases from 1 to 4, the V_{oc} of cells remain at values of around 618 mV, since the V_{oc} of cells is determined by the difference of the Fermi level of the photoelectrode and the redox potential of the electrolyte and is related to the charge recombination process at the photoelectrode, which is without dependence on CoS thickness. The J_{sc} of solar cells drop from 9.41 to 8.43 mA/cm^2; the drop of J_{sc} has been observed elsewhere also when using thicker counter electrode materials.[31] The overall power conversion efficiency is enhanced from 2.19% to 3.19% owing to the increase of fill factor from 38.50% to 60.80%. Further increasing of the CoS layers to five shows no improvement in the cell performances.

The influence of counter electrode on the performance of DSSC is mainly derived from the catalytic ability to regenerate the reduced species (T^-) in the electrolyte as well as the increased conductivity, since it provides easier electron pathways to complete the circuit.[32,33] Electrochemical impedance spectroscopy was introduced to investigate the influence of the CoS thicknesses on the cell performance. Figure 2b shows the Nyquist plots of solar cells applying different layers of CoS as counter electrode and measured under 1 sun at V vs V_{oc}. A typical EIS spectrum of DSSC consists of three semicircles. While the first semicircle responds to the high-frequency, which is attributed to the charge transfer at the counter electrode–electrolyte interface, the second semicircle responds to the middle-frequency, which is attributed to the carrier transport at the photoanode–electrolyte interface, and the third semicircle responds to the low-frequency region attributing to the ion diffusion process in the electrolyte, when the cells are biased at its V_{oc}.[34,35] The second and third semicircles remain the same, since same electrolyte and photoelectrode were used in the solar cells applying different layers of CoS. With the number of CoS layers increasing from one to four, the R_S values, which represents the ohmic series resistance (R_S corresponds to the high frequency intercept of the Nyquist plot), show a diminishing trend. This indicates that the contact resistance between the CoS and FTO gets smaller with an increase in CoS thickness, since the possible discontinuity of thinner CoS film may lead to higher contact resistance.[32] This observation of lower R_s of thicker counter electrode material was also observed elsewhere.[36] The

dx.doi.org/10.1021/am504958f | ACS Appl. Mater. Interfaces 2014, 6, 20768–20775

R_{ct} of the solar cells, which represents the charge transfer resistance at the electrolyte/counter electrode interface (R_{ct} corresponds to the semicircle at the high-frequency range), also decreases with the increasing number of CoS deposition cycles, which is explained by the fact that with thicker CoS deposition, more reduced species regeneration sites are formed, resulting in better catalytic ability of the counter electrode.[33] With the optimized R_s and R_{ct} values, four cycles of CoS as counter electrode material exhibit better catalytic ability and conductivity, thus rationalizing the enhanced solar cell performance. The optimized counter electrode configuration was applied to fabricate cells in the subsequent experiments.

Different concentrations of the TMAT/T_2 compounds were mixed with liquefied SCN at 70 °C, followed by cooling at room temperature to form the quasisolid electrolyte. The melting point of the SCN could be lowered by the addition of salts.[24] As the concentration of the solute increases, a local disorder starts occurring in the plastic crystal, eventually inhibiting the formation of the plastic-crystal phase itself.[24] In this study, various concentrations of TMAT/T_2 compounds were dissolved in SCN to form 0.2/0.2, 0.4/0.2, 0.4/0.4, 0.8/0.4, 0.8/0.8, 1.0/1.0 and 1.2/1.2 M electrolytes. While the 1.0/1.0 M electrolyte exhibits a quasisolid phase, the 1.2/1.2 M sample becomes a highly viscous liquid. The remaining electrolytes present a solid phase at room temperature, as shown in Figure1b; these quasisolid electrolytes were applied to fabricate DSSCs. The $J-V$ characteristics of DSSCs applying electrolyte containing different concentrations of the redox compounds in SCN are presented in Figure 3 and the cell parameters obtained from the $J-V$ curves are listed in Table 2.

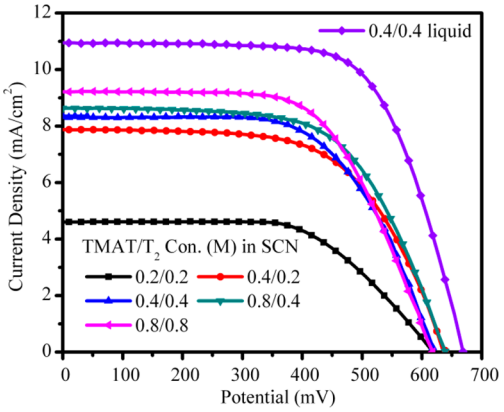

Figure 3. $J-V$ characteristics of DSSCs applied different concentrations of the T^-/T_2 redox couple in SCN.

Table 2. Cell Performance Parameters of DSSCs Applied Electrolyte Containing Different Concentrations of the T^-/T_2 Redox Couple in SCN

solvent	TMAT/T_2 concn (M)	V_{oc} (mV)	J_{sc} (mA/cm^2)	FF (%)	η (%)
acetonitrile	0.4/0.4	671	10.9	66.45	4.90 ± 0.05
succinonitrile	0.2/0.2	618	4.45	60.58	1.66 ± 0.06
	0.4/0.2	639	7.78	62.50	3.12 ± 0.08
	0.4/0.4	618	8.25	62.92	3.21 ± 0.06
	0.8/0.4	640	8.52	62.22	3.39 ± 0.10
	0.8/0.8	618	9.12	62.43	3.52 ± 0.07

According to the data in Table 2, with the increase in the concentrations of the redox compounds, the J_{sc} of cells exhibits an increasing trend, resulting in better overall power conversion efficiencies. Solar cells applying 0.8/0.8 M electrolyte exhibit a J_{sc} = 9.12 mA/cm^2, which show a 100% increase compared to the J_{sc} of cells applying 0.2/0.2 M electrolyte. In a solid or quasisolid electrolyte system, a Grotthuss-type exchange mechanism (GEM) was proposed for ion exchange rather than the mass transportation exhibited in liquid electrolytes, which normally requires higher redox concentrations than that used in liquid electrolytes.[18,37] The higher TMAT/T_2 concentration, 0.8/0.8 M in this case, enables better ion transport through GEM in the electrolyte, which may be attributed to the higher defect concentration in the plastic crystal,[24] thus resulting in higher J_{sc}. Further increase of TMAT/T_2 concentration may lead to even higher defects and thus higher ion diffusion; however, it sacrifices the stability of the plastic crystal, likely to result in a quasisolid or liquid phase, as observed in the 1.0/1.0 and 1.2/1.2 M electrolyte case. The V_{oc} of cells introducing 0.2/0.2, 0.4/0.4, and 0.8/0.8 M electrolyte stay at a same value of 618 mV, while in cells applying 0.4/0.2 and 0.8/0.4 M electrolyte, an increase in V_{oc} of around 20 mV is observed, which can be attributed to the shift of the redox potential of the electrolyte by the change of the oxidized and reduced species' ratio in the electrolyte. The optimized concentration of TMAT/T_2 in succinonitrile is 0.8/0.8 M; cells applying this electrolyte exhibit a V_{oc} of 618 mV, J_{sc} of 9.12 mA/cm^2, FF of 62.43%, and power conversion efficiency of 3.52%. For comparison, a liquid electrolyte employing the reported maximized redox couple concentration (0.4/0.4 M)[8] was also introduced to fabricate cells which shows a power conversion efficiency of 4.90%, with V_{oc} = 671 mV, J_{sc} = 10.9 mA/cm^2, and FF = 66.45%. The performance of the quasisolid DCSSC is lower but comparable to the liquid-electrolyte-based one.

In an effort to further improve the performance of the thiolate/disulfide-based quasisolid DSSC, various additives, including GuSCN, $LiClO_4$, TBP, and NMBI, were added to the electrolyte. As discussed above, high concentrations of solute hinder the formation of the plastic crystal phase; therefore, only a low concentration (0.1 M) of each of the additives was added to the electrolyte. This composition is referred as TMAT/T_2/additive in a proportion of 0.8/0.8/0.1 M. All these electrolytes remained as solids at room temperature. The $J-V$ characteristics of DSSCs applying these additive-containing electrolytes are shown in Figure 4, and the corresponding cell performance parameters are listed in Table 3.

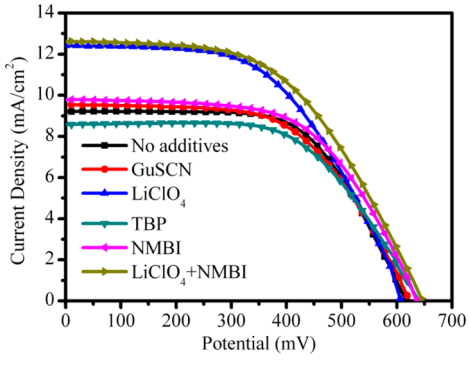

Figure 4. $J-V$ characteristics of DSSCs that applied SCN-based electrolytes containing various additives.

Table 3. SCN-Based Electrolytes: Influence of Various Additives on Cell Parameters

additives	V_{oc} (mV)	J_{sc} (mA/cm^2)	FF (%)	η (%)
none	618	9.12	62.43	3.52 ± 0.07
GuSCN	619	9.45	57.97	3.39 ± 0.03
$LiClO_4$	610	12.4	53.36	4.02 ± 0.09
TBP	639	8.60	59.54	3.27 ± 0.08
NMBI	639	9.73	58.40	3.64 ± 0.05
$LiClO_4$ + NMBI	647	12.6	52.07	4.25 ± 0.07

GuSCN has been reported as an effective additive capable of enhancing both the V_{oc} and J_{sc} of cells, since guanidinium cations adsorbed onto TiO_2 surface enhances the electron injection and suppresses the charge recombination,[38] while the TBP reportedly helps the cell V_{oc} by negatively shifting the TiO_2 conduction band.[38] In our case, the J_{sc} of cells are slightly increased, but FF fell when adding GuSCN, which results in a slightly lower PCE, while the fact of V_{oc} remaining unchanged, as a preliminary guess, may be due the interaction between the guanidinium ions and the redox couple in the electrolyte affecting its redox potential. However, more detailed studies should be done to further investigate this question. TBP, as expected, increased V_{oc} from 618 to 639 mV; however, the increase in V_{oc} is associated with a decrease in J_{sc} and FF, leading to lower overall performance. The $LiClO_4$ additive yielded a remarkable increase in J_{sc} from 9.12 to 12.4 mA/cm^2, which is due to Li cations being coadsorbed onto TiO_2 surface, enhancing electron injection and thus the cell current;[38] even though a lower V_{oc} of 610 mV and FF of 53.36% are observed, an increase in overall cell performance is pronounced with a power conversion efficiency of 4.02%. The adding of NMBI to the electrolyte increases the V_{oc} of cells, following a mechanism similar to that of TBP,[38] along with a slight increase in the J_{sc} as well, resulting in a slightly better overall power conversion efficiency of 3.64%. Since the addition of $LiClO_4$ or NMBI to the electrolyte enhances the cells' overall performance, in the next step both the additives are added in the electrolyte to form a composite of TMAT/T_2/$LiClO_4$/NMBI 0.8/0.8/0.1/0.1 M, respectively. Cells containing this electrolyte exhibit a power conversion efficiency of 4.25% with an increased V_{oc} of 647 mV and J_{sc} of 12.6 mA/cm^2, which are >20% superior compared to cells having electrolytes with no additives.

The observed cell performance enhancement is further investigated by characterizing cells applying electrolyte with $LiClO_4$ + NMBI; cells introducing electrolyte with no additives are used for comparison. Figure 5a shows the dark current density–voltage characteristics of cells applying two kinds of electrolytes. Compared to electrolyte without additives, the electrolyte with $LiClO_4$ + NMBI added shifts the onset of photocurrent to higher voltages and produced a smaller dark current at the same potential above 450 mV, indicating the suppression of electron recombination. The lower recombination rate is mainly attributed to the presence of NMBI in the electrolyte, rationalizing the higher V_{oc}, as observed in Table 3. Figure 5b presented the Nyquist plots of cells introducing electrolyte with and without additives, respectively. In particular, the charge transfer resistance related to the electron transfer process at the TiO_2/dye/electrolyte interface can be determined from the diameter of the central arc in the Nyquist plots.[39] It can be seen that the charge transfer resistance decreases with the addition of $LiClO_4$ + NMBI in the

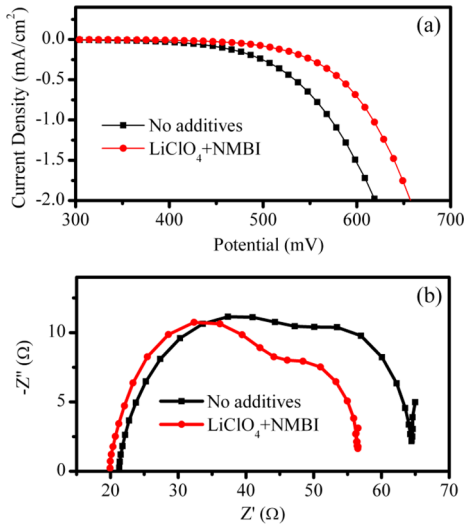

Figure 5. (a) Dark current density–voltage characteristics and (b) Nyquist plots (cells measured at 1 sun illumination at V vs V_{oc}) of cells applying electrolytes without additives and with $LiClO_4$ + NMBI addition.

electrolyte, which may lead to higher electron diffusion and collection efficiency and thus better performance.

Since the arc associated with the electrolyte diffusion was overlapped with the response from the central arc (Figure 5b), in order to understand the effect of additives on the ionic diffusion property of the electrolyte, symmetric cells applying two CoS counter electrode with the two kinds of electrolytes are fabricated and their EIS responses measured. The Nyquist plots obtained are shown in Figure 6a, while the equivalent circuit presented as an inset of Figure 6a is used to fit the Nyquist plots according to a method proposed before.[40] In the Nyquist plots, the responses at high frequency are associated with the counter electrode/electrolyte interface, while the arcs at the lower frequencies are related to the ionic diffusion process in the electrolyte. From the parameters attained by

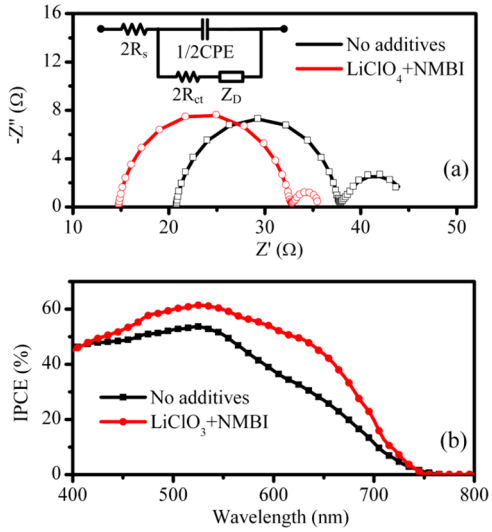

Figure 6. (a) Nyquist plots of symmetric cells applying CoS counter electrode and electrolyte with no additives and with $LiClO_4$ + NMBI (cells measured under dark at V = 0 V vs E_{ref}; the solid lines represent experimental results, while hollow dots indicate the simulated values) and (b) IPCE values of cells applying two kinds of electrolytes.

dx.doi.org/10.1021/am504958f | ACS Appl. Mater. Interfaces 2014, 6, 20768–20775

fitting the Nyquist plots, the apparent diffusion coefficient of ionic species in the electrolyte can be estimated using the equation $D = l_e^2/B^2$, where l_e is the thickness of the electrolyte film and B is a parameter related to the element representing the electrolyte diffusion process in the equivalent circuit, which accounts for a finite length Warburg diffusion (Z_D).

The apparent diffusion coefficient of ionic species in the electrolyte with $LiClO_4$ + NMBI is estimated to be 3.2×10^{-6} cm^2 s^{-1}, much higher than the diffusion coefficient estimated for the electrolyte with no additives (1.9×10^{-6} cm^2 s^{-1}). The value obtained is quite close to the diffusion coefficient for ionic species in highly viscous solvents (2.8×10^{-6} cm^2 s^{-1}),[41] in gel (3×10^{-6} cm^2 s^{-1}),[42] or in gellified ionic liquids (1.4×10^{-6} cm^2 s^{-1}),[43] but it is still 1 order of magnitude lower than that in acetonitrile (around 2×10^{-5} cm^2 s^{-1}).[44] A higher diffusion coefficient of ionic species is normally related to a higher ionic conductivity of the electrolyte. Thus, with a promising apparent diffusion coefficient of ionic species in the electrolyte, plus a reduced electron transfer resistance, a higher J_{sc} is reasonable to be obtained for cells applying electrolyte with $LiClO_4$ + NMBI. The observation of the higher J_{sc} is also consistent with the difference in IPCE values obtained from cells applying two kinds of electrolytes (Figure 6b).

Solar cells introducing the optimized electrolyte (TMAT/T_2/$LiClO_4$/NMBI 0.8/0.8/0.1/0.1 M) are then characterized under AM 1.5G at various light intensities. The respective $J-V$ characteristics are presented in Figure 7, and the cell parameters

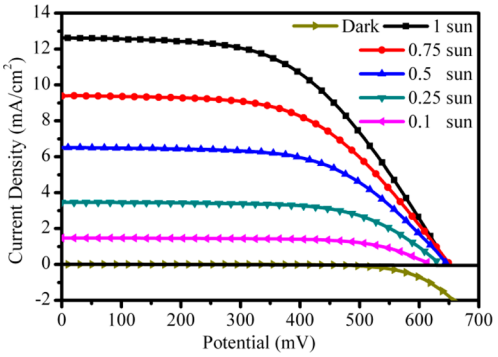

Figure 7. $J-V$ characteristics of DSSCs applying the optimized solid electrolyte at varied light intensities.

Table 4. Cell Performance Parameters Obtained from $J-V$ Measurements of DSSCs Applying the Maximized Solid Electrolyte at Different Light Intensities

light intensity (sun)	V_{oc} (mV)	J_{sc} (mA/cm²)	FF (%)	η (%)
1	645	12.6	52.37	4.26
0.75	649	9.41	54.70	4.45
0.5	645	6.50	58.53	4.91
0.25	629	3.46	64.32	5.60
0.1	613	1.47	68.42	6.19

are summarized in Table 4. Under lower light intensities, cells show improved overall behavior. At 0.1 sun, a maximum efficiency value of 6.19% was obtained with a V_{oc} of 613 mV, J_{sc} of 1.47 mA/cm^2, and FF of 68.42%. The better performance of the device under lower light intensity may be due to the more efficient charge screening of electrons[19] and less diffusion overpotential,[45] thus improving both the J_{sc} and FF. There was also a study suggesting that it is more effective to use an electrolyte system with higher transparency than fast ion diffusion rate under low light intensities;[45] thus, the performance of cells applying the highly transparent thiolate/disulfide electrolyte should be reasonably more efficient under low light intensities. The promising performance under lower light intensities indicated the potential utilization of this quasisolid electrolyte in DSSCs featuring indoor applications.

In one of our other reports,[46] a thiolate/disulfide-based liquid electrolyte was successfully applied in CdS QDSSCs. Cells applying electrolyte containing 0.4/0.4 M of TMAT/T_2 in acetonitrile, CdS QD-sensitized TiO_2 working electrode, and a platinum counter electrode exhibited a power conversion efficiency of 0.83%. In this work, the maximized quasisolid electrolyte has been put to the test with CdS in QDSSCs. CdS QDs were deposited on TiO_2 films using the SILAR technique. The benchmark of seven SILAR cycles of CdS deposition, a strategy derived from previous work, was applied followed by the ZnS passivation process.[47] All solid CdS QDSSCs are fabricated by introducing the CdS-sensitized photoelectrode, the maximized quasisolid electrolyte, and the CoS counter electrode. A power conversion efficiency of 0.94% was obtained from the best cell with a V_{oc} of 588 mV, J_{sc} of 3.06 mA/cm^2, and FF of 52.15%. The $J-V$ characteristic of the cell is presented in Figure 8. The cell efficiency is limited by the

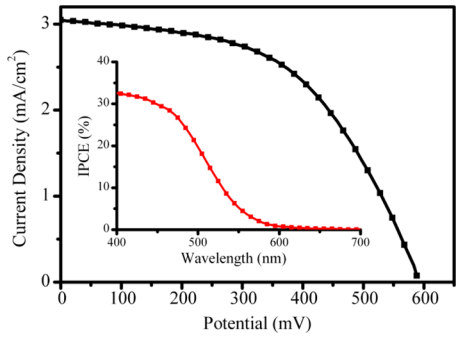

Figure 8. $J-V$ characteristic of quasisolid CdS QDSSC (inset shows the IPCE values).

relatively low J_{sc}, which is obviously due to the low IPCE of around 30% measured (inset of Figure 8) and the limited range of absorbance that is possible by CdS QDs. However, the result is not bad when compared with quasisolid CdS QDSSCs results reported when applying Spiro-OMeTAD (power conversion efficiency of 0.2%,[48] 0.8%[49]) or P3HT hole-conductors (1.4%[50]). Compared to the spiro compound and P3HT, the present electrolyte is much more stable and adaptable to the ambient atmospheric conditions; it is also less expensive. With a concerted effort, this electrolyte could therefore be better used in QDSSC quasisolid cells, especially when QDs with a much wider absorption range than CdS are used.

4. CONCLUSION

To conclude, a room temperature quasisolid electrolyte based on a thiolate/disulfide redox couple in succinonitrile matrix has been developed. Mesoporous TiO_2-based DSSCs fabricated using this novel quasisolid electrolyte and compatible CoS counter electrodes showed promising power conversion efficiencies. The composition of the electrolyte is maximized by tuning the concentration of the redox compounds and other

additives. *J*–*V*, EIS, and IPCE measurements were conducted to evaluate the hole-collection and charge mediator properties. The maximized device exhibited an overall power conversion efficiency of 4.26% under AM 1.5G illumination at 1 sun and 6.19% at 0.1 sun. The optimized electrolyte, when introduced into CdS QDSSCs, a material with a limited light absorption range, manifested a promising power conversion efficiency of 0.94%. The results indicate the potential of using the novel quasisolid ionic conductor to fabricate highly efficient sensitized solar cells, especially at low light intensities.

■ ASSOCIATED CONTENT

Ⓢ Supporting Information

Figure S1, showing pictures of a thin quasisolid electrolyte layer, along with relevant experimental details. This material is available free of charge via the Internet at http://pubs.acs.org/.

■ AUTHOR INFORMATION

Corresponding Author

*Fax: +35317161177. Tel: +35317161995. E-mail: ravindranathan.thampi@ucd.ie.

Notes

The authors declare no competing financial interest.

■ ACKNOWLEDGMENTS

K.R.T. acknowledges the SFI-Airtricity Stokes professorship grant. K.M. acknowledges the funding support received from China Scholarship Council.

■ REFERENCES

(1) Grätzel, M. Dye-Sensitized Solar Cells. *J. Photochem. Photobiol., C* **2003**, *4*, 145–153.
(2) Rühle, S.; Shalom, M.; Zaban, A. Quantum-Dot-Sensitized Solar Cells. *ChemPhysChem* **2010**, *11*, 2290–2304.
(3) Kamat, P. V. Quantum Dot Solar Cells. Semiconductor Nanocrystals as Light Harvesters. *J. Phys. Chem. C* **2008**, *112*, 18737–18753.
(4) Nazeeruddin, M. K.; Kay, A.; Rodicio, I.; Humphry-Baker, R.; Müller, E.; Liska, P.; Vlachopoulos, N.; Grätzel, M. Conversion of Light to Electricity by *cis*-X_2Bis(2,2′-bipyridyl-4,4′-dicarboxylate)-ruthenium(II) Charge-Transfer Sensitizers (X = Cl^-, Br^-, I^-, CN^-, and SCN^-) on Nanocrystalline Titanium Dioxide Electrodes. *J. Am. Chem. Soc.* **1993**, *115*, 6382–6390.
(5) Ito, S.; Nazeeruddin, M.; Liska, P.; Comte, P.; Charvet, R.; Péchy, P.; Jirousek, M.; Kay, A.; Zakeeruddin, S. M.; Grätzel, M. Photovoltaic Characterization of Dye-Sensitized Solar Cells: Effect of Device Masking on Conversion Efficiency. *Prog. Photovoltaics* **2006**, *14*, 589–601.
(6) Daeneke, T.; Kwon, T.-H.; Holmes, A. B.; Duffy, N. W.; Bach, U.; Spiccia, L. High-Efficiency Dye-Sensitized Solar Cells with Ferrocene-Based Electrolytes. *Nat. Chem.* **2011**, *3*, 211–215.
(7) Wang, M.; Grätzel, C.; Zakeeruddin, S. M.; Grätzel, M. Recent Developments in Redox Electrolytes for Dye-Sensitized Solar Cells. *Energy Environ. Sci.* **2012**, *5*, 9394–9405.
(8) Wang, M.; Chamberland, N.; Breau, L.; Moser, J. E.; Humphry-Baker, R.; Marsan, B.; Zakeeruddin, S. M.; Grätzel, M. An Organic Redox Electrolyte to Rival Triiodide/Iodide in Dye-Sensitized Solar Cells. *Nat. Chem.* **2010**, *2*, 385–389.
(9) Xu, X.; Cao, K.; Huang, D.; Shen, Y.; Wang, M. Disulfide/thiolate Based Redox Shuttle for Dye-Sensitized Solar Cells: An Impedance Spectroscopy Study. *J. Phys. Chem. C* **2012**, *116*, 25233–25241.
(10) Burschka, J.; Brault, V.; Ahmad, S.; Breau, L.; Nazeeruddin, M. K.; Marsan, B.; Zakeeruddin, S. M.; Grätzel, M. Influence of the Counter Electrode on the Photovoltaic Performance of Dye-Sensitized Solar Cells Using a Disulfide/Thiolate Redox Electrolyte. *Energy Environ. Sci.* **2012**, *5*, 6089–6097.
(11) Liu, G.; Li, X.; Wang, H.; Rong, Y.; Ku, Z.; Xu, M.; Liu, L.; Hu, M.; Yang, Y.; Han, H. An Efficient Thiolate/disulfide Redox Couple Based Dye-Sensitized Solar Cell with a Graphene Modified Mesoscopic Carbon Counter Electrode. *Carbon* **2013**, *53*, 11–18.
(12) Wu, H.; Lv, Z.; Hou, S.; Cai, X.; Wang, D.; Kafafy, H.; Fu, Y.; Zhang, C.; Chu, Z.; Zou, D. A New Ionic Liquid Organic Redox Electrolyte for High-Efficiency Iodine-Free Dye-Sensitized Solar Cells. *J. Power Sources* **2013**, *221*, 328–333.
(13) Tian, H.; Gabrielsson, E.; Yu, Z.; Hagfeldt, A.; Kloo, L.; Sun, L. A Thiolate/Disulfide Ionic Liquid Electrolyte for Organic Dye-Sensitized Solar Cells Based on Pt-Free Counter Electrodes. *Chem. Commun.* **2011**, *47*, 10124–10126.
(14) Li, B.; Wang, L.; Kang, B.; Wang, P.; Qiu, Y. Review of Recent Progress in Solid-State Dye-Sensitized Solar Cells. *Sol. Energy Mater. Sol. Cells* **2006**, *90*, 549–573.
(15) Chung, I.; Lee, B.; He, J.; Chang, R. P.; Kanatzidis, M. G. All-Solid-State Dye-Sensitized Solar Cells with High Efficiency. *Nature* **2012**, *485*, 486–489.
(16) Fabregat-Santiago, F.; Bisquert, J.; Cevey, L.; Chen, P.; Wang, M.; Zakeeruddin, S. M.; Grätzel, M. Electron Transport and Recombination in Solid-State Dye Solar Cell with Spiro-OMeTAD as Hole Conductor. *J. Am. Chem. Soc.* **2008**, *131*, 558–562.
(17) Byrne, O.; Coughlan, A.; Surolia, P. K.; Thampi, K. R. Succinonitrile-Based Solid-State Electrolytes for Dye-Sensitised Solar Cells. *Prog. Photovoltaics* **2013**, DOI: 10.1002/pip.2441.
(18) Hwang, D.; Kim, D. Y.; Jo, S. M.; Armel, V.; MacFarlane, D. R.; Kim, D.; Jang, S.-Y. Highly Efficient Plastic Crystal Ionic Conductors for Solid-State Dye-Sensitized Solar Cells. *Sci. Rep.* **2013**, *3*, 3520.
(19) Wang, P.; Dai, Q.; Zakeeruddin, S. M.; Forsyth, M.; MacFarlane, D. R.; Grätzel, M. Ambient Temperature Plastic Crystal Electrolyte for Efficient, All-Solid-State Dye-Sensitized Solar Cell. *J. Am. Chem. Soc.* **2004**, *126*, 13590–13591.
(20) Derollez, P.; Lefebvre, J.; Descamps, M.; Press, W.; Fontaine, H. Structure of Succinonitrile in Its Plastic Phase. *J. Phys.: Condens. Matter* **1990**, *2*, 6893.
(21) Dai, Q.; MacFarlane, D. R.; Forsyth, M. High Mobility I^-/I_3^- Redox Couple in a Molecular Plastic Crystal: A Potential New Generation of Electrolyte for Solid-State Photoelectrochemical Cells. *Solid-State Ionics* **2006**, *177*, 395–401.
(22) MacFarlane, D. R.; Huang, J.; Forsyth, M. Lithium-Doped Plastic Crystal Electrolytes Exhibiting Fast Ion Conduction for Secondary Batteries. *Nature* **1999**, *402*, 792–794.
(23) Hawthorne, H.; Sherwood, J. Lattice Defects in Plastic Organic Crystals. Part 3—Plastic Deformation in Pure and Impure Camphene. *Trans. Faraday Soc.* **1970**, *66*, 1799–1801.
(24) Alarco, P.-J.; Abu-Lebdeh, Y.; Abouimrane, A.; Armand, M. The Plastic-Crystalline Phase of Succinonitrile as a Universal Matrix for Solid-State Ionic Conductors. *Nat. Mater.* **2004**, *3*, 476–481.
(25) Hwang, D.; Jo, S. M.; Kim, D. Y.; Armel, V.; MacFarlane, D. R.; Jang, S.-Y. High-Efficiency, Solid-State, Dye-Sensitized Solar Cells Using Hierarchically Structured TiO_2 Nanofibers. *ACS Appl. Mater. Interfaces* **2011**, *3*, 1521–1527.
(26) De Rossi, F.; Di Gaspare, L.; Reale, A.; Di Carlo, A.; Brown, T. Blending CoS and Pt for Amelioration of Electrodeposited Transparent Counterelectrodes and the Efficiency of Back-Illuminated Dye Solar Cells. *J. Mater. Chem. A* **2013**, *1*, 12941–12947.
(27) Yang, Z.; Chen, C. Y.; Liu, C. W.; Li, C. L.; Chang, H. T. Quantum Dot–Sensitized Solar Cells Featuring CuS/CoS Electrodes Provide 4.1% Efficiency. *Adv. Energy Mater.* **2011**, *1*, 259–264.
(28) Yang, J.; Bao, C.; Zhu, K.; Yu, T.; Li, F.; Liu, J.; Li, Z.; Zou, Z. High Catalytic Activity and Stability of Nickel Sulfide and Cobalt Sulfide Hierarchical Nanospheres on the Counter Electrodes for Dye-Sensitized Solar Cells. *Chem. Commun.* **2014**, *50*, 4824–4826.
(29) Ito, S.; Chen, P.; Comte, P.; Nazeeruddin, M. K.; Liska, P.; Pechy, P.; Grätzel, M. Fabrication of Screen-Printing Pastes from TiO_2 Powders for Dye-Sensitised Solar Cells. *Prog. Photovoltaics* **2007**, *15*, 603–612.

(30) Meng, K.; Surolia, P. K.; Byrne, O.; Thampi, K. R. Efficient CdS Quantum Dot Sensitized Solar Cells Made Using Novel Cu_2S Counter Electrode. *J. Power Sources* **2014**, *248*, 218−223.
(31) Han, J.; Yoo, K.; Ko, M.; Yu, B.; Noh, Y.; Song, O. Effect of the Thickness of the Ru-Coating on a Counter Electrode on the Performance of a Dye-Sensitized Solar Cell. *Met. Mater. Int.* **2012**, *18*, 105−108.
(32) Lee, L. T. L.; He, J.; Wang, B.; Ma, Y.; Wong, K. Y.; Li, Q.; Xiao, X.; Chen, T. Few-Layer $MoSe_2$ Possessing High Catalytic Activity towards Iodide/Tri-Iodide Redox Shuttles. *Sci. Rep.* **2014**, *4*, 4063.
(33) Fang, X.; Ma, T.; Guan, G.; Akiyama, M.; Abe, E. Performances Characteristics of Dye-Sensitized Solar Cells Based on Counter Electrodes with Pt Films of Different Thickness. *J. Photochem. Photobiol., A* **2004**, *164*, 179−182.
(34) Li, G. r.; Wang, F.; Jiang, Q. w.; Gao, X. p.; Shen, P. w. Carbon Nanotubes with Titanium Nitride as a Low-Cost Counter-Electrode Material for Dye-Sensitized Solar Cells. *Angew. Chem., Int. Ed.* **2010**, *49*, 3653−3656.
(35) Fabregat-Santiago, F.; Bisquert, J.; Garcia-Belmonte, G.; Boschloo, G.; Hagfeldt, A. Influence of Electrolyte in Transport and Recombination in Dye-Sensitized Solar Cells Studied by Impedance Spectroscopy. *Sol. Energy Mater. Sol. Cells* **2005**, *87*, 117−131.
(36) Ye, M.; Zheng, D.; Wang, M.; Chen, C.; Liao, W.; Lin, C.; Lin, Z. Hierarchically Structured Microspheres for High-Efficiency Rutile TiO_2-Based Dye-Sensitized Solar Cells. *ACS Appl. Mater. Interfaces* **2014**, *6*, 2893−2901.
(37) Cao, Y.; Zhang, J.; Bai, Y.; Li, R.; Zakeeruddin, S. M.; Grätzel, M.; Wang, P. Dye-Sensitized Solar Cells with Solvent-Free Ionic Liquid Electrolytes. *J. Phys. Chem. C* **2008**, *112*, 13775−13781.
(38) Yu, Z.; Vlachopoulos, N.; Gorlov, M.; Kloo, L. Liquid Electrolytes for Dye-Sensitized Solar Cells. *Dalton Trans.* **2011**, *40*, 10289−10303.
(39) Bai, Y.; Xing, Z.; Yu, H.; Li, Z.; Amal, R.; Wang, L. Porous Titania Nanosheet/Nanoparticle Hybrids as Photoanodes for Dye-Sensitized Solar Cells. *ACS Appl. Mater. Interfaces* **2013**, *5*, 12058−12065.
(40) De Freitas, J. N.; Nogueira, A. F.; De Paoli, M.-A. New Insights into Dye-Sensitized Solar Cells with Polymer Electrolytes. *J. Mater. Chem.* **2009**, *19*, 5279−5294.
(41) Papageorgiou, N.; Grätzel, M.; Infelta, P. P. On the Relevance of Mass Transport in Thin Layer Nanocrystalline Photoelectrochemical Solar Cells. *Sol. Energy Mater. Sol. Cells* **1996**, *44*, 405−438.
(42) Dürr, M.; Kron, G.; Rau, U.; Werner, J.; Yasuda, A.; Nelles, G. Diffusion-Limited Transport of I_3^- through Nanoporous TiO_2-Polymer Gel Networks. *J. Chem. Phys.* **2004**, *121*, 11374−11378.
(43) Wang, P.; Zakeeruddin, S. M.; Comte, P.; Exnar, I.; Grätzel, M. Gelation of Ionic Liquid-Based Electrolytes with Silica Nanoparticles for Quasi-Solid-State Dye-Sensitized Solar Cells. *J. Am. Chem. Soc.* **2003**, *125*, 1166−1167.
(44) Kebede, Z.; Lindquist, S.-E. The Obstructed Diffusion of the I_3^- Ion in Mesoscopic TiO_2 Membranes. *Sol. Energy Mater. Sol. Cells* **1998**, *51*, 291−303.
(45) Lan, J.-L.; Wei, T.-C.; Feng, S.-P.; Wan, C.-C.; Cao, G. Effects of Iodine Content in the Electrolyte on the Charge Transfer and Power Conversion Efficiency of Dye-Sensitized Solar Cells under Low Light Intensities. *J. Phys. Chem. C* **2012**, *116*, 25727−25733.
(46) Meng, K.; Surolia, P.; Byrne, O.; Thampi, K. R. Quantum Dot and Quantum Dot-Dye Co-Sensitized Solar Cells Containing Organic Thiolate−Disulfide Redox Electrolyte. *J. Power Sources* **2014**. DOI: 10.1016/j.jpowsour.2014.11.064.
(47) Meng, K.; Surolia, P.; Thampi, K. R. $BaTiO_3$ Photoelectrodes for CdS Quantum Dot Sensitized Solar Cells. *J. Mater. Chem. A* **2014**, *2*, 10231−10238.
(48) Brennan, T. P.; Ardalan, P.; Lee, H. B. R.; Bakke, J. R.; Ding, I.; McGehee, M. D.; Bent, S. F. Atomic Layer Deposition of CdS Quantum Dots for Solid-State Quantum Dot Sensitized Solar Cells. *Adv. Energy Mater.* **2011**, *1*, 1169−1175.
(49) Lee, H. J.; Leventis, H. C.; Moon, S. J.; Chen, P.; Ito, S.; Haque, S. A.; Torres, T.; Nüesch, F.; Geiger, T.; Zakeeruddin, S. M. PbS and CdS Quantum Dot-Sensitized Solid-State Solar Cells: "Old" Concepts, New Results. *Adv. Funct. Mater.* **2009**, *19*, 2735−2742.
(50) Qian, J.; Liu, Q.-S.; Li, G.; Jiang, K.-J.; Yang, L.-M.; Song, Y. P3HT as Hole Transport Material and Assistant Light Absorber in CdS Quantum Dots-Sensitized Solid-State Solar Cells. *Chem. Commun.* **2011**, *47*, 6461−6463.